INTERNATIONAL JOURNAL OF Telecommunications AIR DEFENSE COLLEGE

DC Motor Emulation of Wind Energy Conversion System

H. M. N. Fiyad [1,*], Wael. M. Mokhtar [2], and Ehab Mohamed Ali [3]

Citation: Fiyad, H. M. N.; Mokhtar, W. M.; Ali, E. M. *International Journal of Telecommunications, IJT'2021, Vol. 01, Issue 01, pp. 1-8, December 2021.* https://ijt-adc.org/articles/2805-3044/665619

Editor-in-Chief: Yasser M. Madany

Received: 31-10-2021

Accepted: 2-12-2021

Published: 26-12-2021

Publisher's Note: The International Journal of Telecommunications, IJT, stays neutral regarding jurisdictional claims in published maps and institutional affiliations.

[1] Air Defense Collage, Alexandria University, Alexandria, Egypt; hfiyad098@yahoo.com.
[2] Air Defense Collage, Alexandria University, Alexandria, Egypt; Waelm_1970@yahoo.com.
[3] Air Defense Collage, Alexandria University, Alexandria, Egypt; ehab.ali.7510m.adc@alexu.edu.eg.
* Correspondence: hfiyad098@yahoo.com.

Abstract: This paper presents a novel current control technique to control a separately excited DC motor in order to emulate the Wind Energy Conversion System (WECS) experimentally. This system is utilized to simulate the dynamic behaviors of WECS accurately in extension to a wide range of operating conditions. The suggested system is carried out in the laboratory using a set of separately excited DC motor, permeant magnet synchronous generator, Half-controlled rectifier bridge, firing circuit of the DC motor half-controlled rectifier bridge, current sensor, voltage sensor, speed sensor and a controller. Nonlinear model of WECS is derived and studied in addition to the operation of WECS at maximum mechanical power. DC motor current, voltage and speed are sensed using a set of predesigned sensors in order to feedback the system and record results. Experimental test results of the suggested wind energy conversion system are listed in static and dynamic cases to investigate the effectiveness for applying the suggested control technique to the developed system.

Keywords: Wind Turbine Emulator (WTE); Wind Energy Conversion System (WECS); Permanent Magnet Synchronous Motor (PMSM); Kinetic Energy (K.E.); Digital Signal Processor (DSP); Doubly Fed Induction Generator (DFIG).

1. Introduction

Electrical energy generation from the wind is the most cost competitive of all the environmental clean and safe sources of renewable energy in the world. Wind power can contribute to fulfilling several of national environmental quality objectives, and the continued expansion of wind power is of strategic importance [1,2]. Wind speed has varying values and directions, so this problem makes it difficult to regulate the output power value from the WECS. To overcome this problem a set of control circuit and different control methods are used to modify the output power value from the generator to be usable either as a DC or AC source of power [3]. A rectifier bridge is utilized to rectify the generator AC output voltage to supply either DC loads or charging batteries [4, 5]. The output power value from the rectifier bridge can be fed to an inverter to be modified as an AC source [6-9]. The best usage of this system is considered in remote areas [10-12] and can be connected to the utility grid to shares loads with the grid. Small-scale stand-alone wind energy is increasingly viewed as a viable and sometimes preferred source of electrical energy. Consider, for example, remote villages in developing countries or ranches located far away from main power lines. Wind energy is a quiet alternative to remote diesel generation that sometimes depends on excessive transportation and fuel storage costs, and an economically justifiable alternative to a grid connection. Wind Turbines (WT) may be operated either at constant speed or at variable speed, for a constant-speed WT, the generator is directly connected to the utility grid, while with variable speed WT electronic equipment are used to control the generators output. There are several reasons for using variable speed operations of wind turbine among those are [13]:

1. Possibilities to reduce stresses of the mechanical structure.

2. Acoustic noise reduction.
3. Possibilities to control reactive and active power.

A real wind turbine may not always be available for R&D so the provision of a controllable experimental platform without reliance on natural wind resources is very important. WTE is equipment for developing WECS used for research applications [14]. WTE drives an electrical generator in a similar way as a Wind Turbine, by reproducing the torque developed for a given wind velocity Also, it can be used as an educational tool to teach the behavior, operation and control of a WT. Over the past years a lot of research has been made on WTE in which different kinds of prime movers have been used in realizing WTE. DC motors produces most of the mechanical movement in the world as they convert electrical energy in DC form to mechanical energy. Due to its simple operation and control and due to its availability at wide range of ratings it has been chosen for simulating wind in the wind turbine system [15]. The DC motor is easy to implement, so most of the WTE are based on separately excited DC machine [16].

An experimental structure that consists of a WT model, with a separately excited DC motor coupled to a Permanent Magnet Synchronous Generator (PMSG) to emulate WT rotor speed is presented in detail. W. LI et al also utilized DC motor but joined to Doubly Fed Induction Generator (DFIG) with a control application generated using C-language and achieved utilizing Digital Signal Processor (DSP), which creates the speed or torque signals to a DC drive through a digital-to-analog converter [17]. The frequency demand values, and armature current were controlled in such a way that the inverter-controlled shaft generated the steady-state properties of a constant step WT. Brushless DC motor and Permanent Magnet Synchronous motor (PMSM) are also utilized as prime movers for implementing WTE [18].

This paper provides to design a WE coupled to 2 kW PMSG for WECS. The turbine torque and rotation are both simulated according to wind speed and load conditions. A detailed description of Wind Emulator along with simulation. The experimental outcomes are shown in following sections.

2. Nonlinear Model of WECS

The kinetic Energy stored in the air stream is:

$$K.E. = \frac{1}{2}mV^2 \tag{1}$$

where:

m : Mass of incoming air (kg).

V : Velocity of the wind (m/s).

Since power is energy per unit time, the power represented by a mass of air moving with velocity V through area A will be Power through area A as:

$$A = \frac{Energy}{Time} = \frac{1}{2}\left(\frac{m}{Time}\right)V^2 \tag{2}$$

The mass flow rate ṁ, through area A, is the product of air density ρ, speed V and cross-sectional area A:

$$\left(\frac{m\ passing\ through\ A}{Time}\right) = \dot{m} = \rho AV \tag{3}$$

Thus

$$P_w = \frac{1}{2}\rho AV^3 \tag{4}$$

where:

A : Frontal area of the wind turbine in(m^2).

P_w: The power of the wind measured in (Watt).

ρ : The density of dry air = 1.225 measured in (kg/m^3) at average atmospheric pressure at sea level and at (15° C).

V : The velocity of the wind measured in (m/s).

R : The radius of the rotor measured in (m).

The above equation shows that the available power in the wind is relatively to the air density, cross sectional area of air stream, and the cube of wind speed. Actually, the power available in the wind is not completely captured by the turbine. A coefficient used to define the ratio between the mechanical output powers of the turbine to available wind power.

$$C_p = P_m/P_w \tag{5}$$

And so,

$$P_m = \frac{1}{2}\rho A C_p V^3 \tag{6}$$

where C_p is known as the power coefficient and is a function of turbines blade tip speed to wind speed ratio λ, and blade pitch angle β, $C_p f(\lambda \& \beta)$:

$$\lambda = \omega_t R/V \tag{7}$$

where:
R : Radius of wind turbine.
ω_t : Angular speed of the wind turbine $= 2\pi N$.
N : Turbine wheel revolution per unit time.
V : The velocity of the wind measured in (m/s).
The relation between $C_p$and λ is plotted in **Figure**.1.

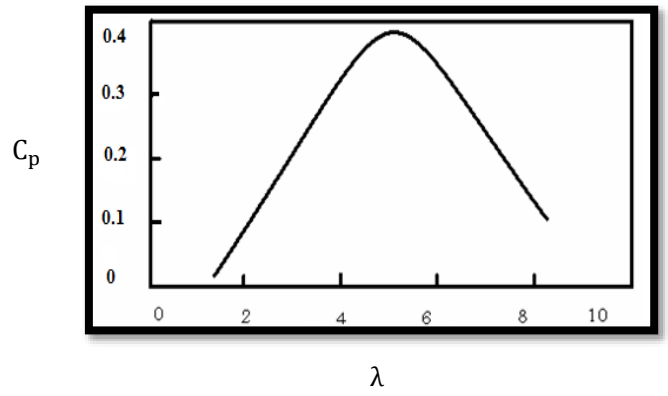

Figure 1. Relation between $C_p$and λ

From Figure1, there is a maximum value of C_p and so a maximum power could be extracted from the wind. Also, there is a value of λ at which C_p has a maximum value, if the turbine speed is allowed to vary such that the value of λ is kept constant at the value corresponding to C_{pmax}, then maximum output power could be obtained.

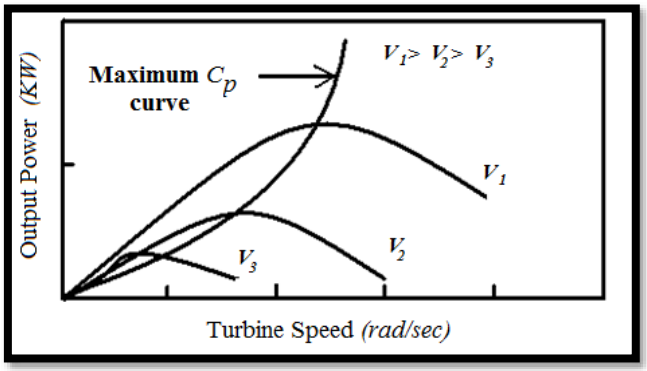

Figure 2. Relation between turbine speed and output power

Figure.2 shows the relation between the output power and rotor speed for different wind speeds (V_1, V_2, V_3). From figures 1 and 2, at every wind speed the maximum power occurs at the point of maximum C_p (if we connect the maximum point at every wind speed curve this line is called maximum C_p curve. By tracking the line that passes through C_{pmax} for different wind speeds we can maximize the output power from the wind turbine), which is shown in Figure.2.

3. DC Motor Emulation of Wind Turbine

Emulation of the WT characteristics can be achieved by using DC motor. For certain wind speed the computer program calculates the mechanical power. Electrical power could be calculated according to the efficiency of WT. Electrical torque can be calculated utilizing the measured motor speed. Reference current is calculated by using torque constant of the DC motor. Finally, the firing angles of the bridge thyristors are calculated using a closed loop current control of the DC motor armature circuit. This manner is performed each sample by using digital control system described in Figure.3.

A separately exited DC motor is used to simulate the properties of the WT. Controlling the armature current of the DC motor can be used to have the same power versus rotor speed characteristics of the wind turbine. **Figure**.3 shows the functional block diagram of the laboratory simulator of the wind turbine using a DC motor with current control technique. A PI controller is utilized for controlling the armature current, this controller is achieved with a digital computer. The instants of the firing pulses of the half-controlled rectifier bridge are controlled by the controlling voltage (V_C) that comes out from the interfacing card.

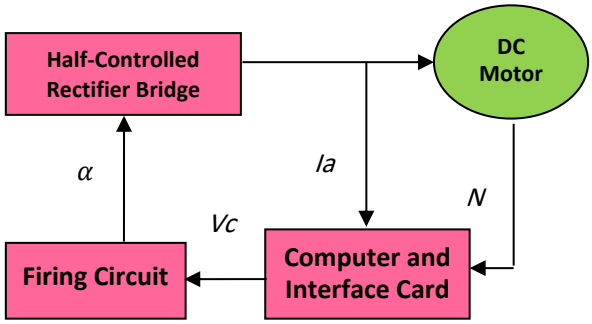

Figure 3. Functional block diagram of DC motor emulation

A single-phase half-controlled rectifier bridge is used to supply the DC motor with a variable DC voltage. This can be achieved by using a reliable firing circuit. Figure.4 shows a photograph of the whole circuit of the half-controlled rectifier bridge used in controlling the DC motor. It consists of power supply, firing circuit, and control circuit. This circuit was constructed in the laboratory and used in converting AC to DC, feeding the DC motor whose parameters are listed in Table.1.

Table 1. DC motor parameters

parameters	values
Nominal armature voltage (V)	220
Nominal current (A)	20
Output power (KW)	4
Rotor speed (rpm)	1500
Field voltage (V)	100
Field current (A)	0.65

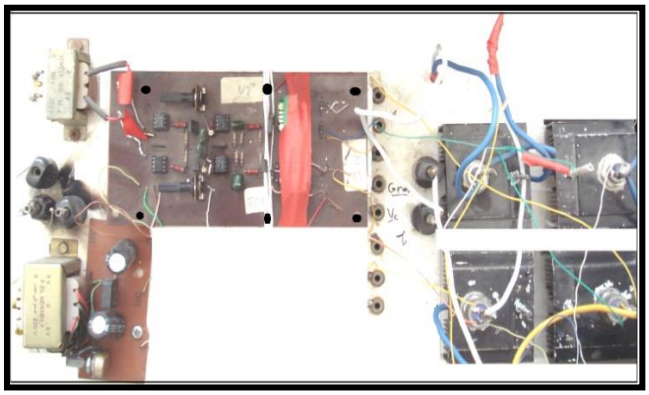

Figure 4. Half-controlled rectifier bridge circuit

Figure.5 shows the circuit diagram of the power circuit of the half-controlled rectifier that consists of two diodes and two thyristors which used to generate the voltage required to control the DC motor. Figure.6 shows the firing circuit that produces the necessary pulses to trigger the rectifier's thyristors. The delay of the pulses is determined by the computer.

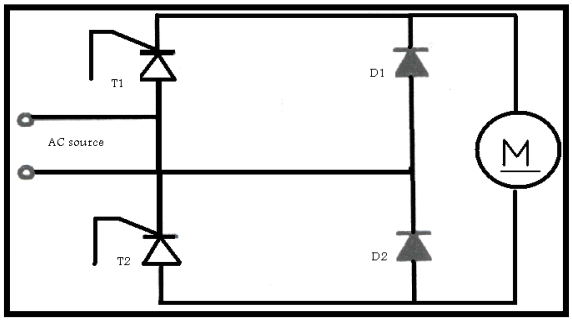

Figure 5. A single-phase half-controlled rectifier bridge

The firing circuit consists of the following parts:

4. Zero Crossing Detector (ZCD).
5. Ramp generator.
6. Comparator.
7. Differentiator.
8. Opti solation Stage.

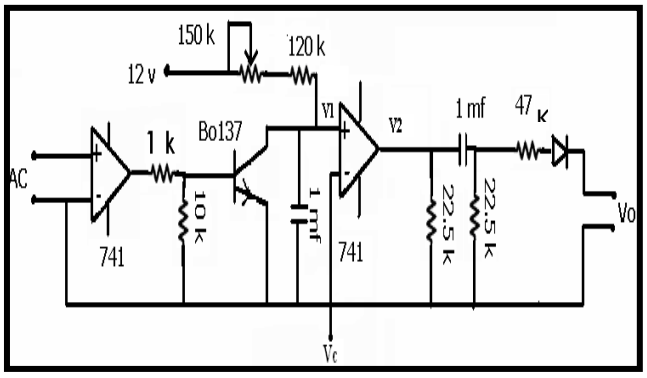

Figure 6. Firing circuit for half-controlled bridge rectifier

The function of zero crossing detector (Z.C.D) is to detect the instant at which the sine waves equal zero. The circuit uses an operational amplifier. The input to the non-inverting terminal is the sine wave and this value is

compared to the ground voltage at the inverting terminal. The output from the operational amplifier is a square wave swinging between positive saturation of +12 volts and negative saturation of -12 volts.
Two zero crossing detectors are used with a phase shift of 180° between them. This phase shift is achieved by applying the sine wave to the inverting terminal of the second amplifier. The output signal from the zero-crossing detector is changed into a ramp shaped wave form. It consists of an RC-circuit shunted with a transistor. The value of the charging time of the capacitor is determined by the value of the resistance and capacitance; appropriate values are shown in Figure.6.
The output of the ramp generator (V_{01}) is compared with a controlling voltage (V_0). When the voltage of the ramp generator (V_0) is greater than the controlling voltage (V_0) the output of the comparator (V_{02}) is positive saturation voltage and vice versa.
The differentiator is used to produce the gate pulses of the thyristors. The isolation stage is used to isolate the rectifier power circuit from the electronic firing circuit. It protects the elements of the firing circuit and computer with the interfacing card from any fault in the power circuit and isolates the gates of the thyristors from each other.

4. Experimental Results

4.1. Constant wind speed test

In this case, a constant wind speed is applied to the whole test period. Figure.7 shows the test result for a 10 m/sec wind speed as well as corresponding response of the rotor speed, DC motor current, control voltage, DC link current and DC link voltage.

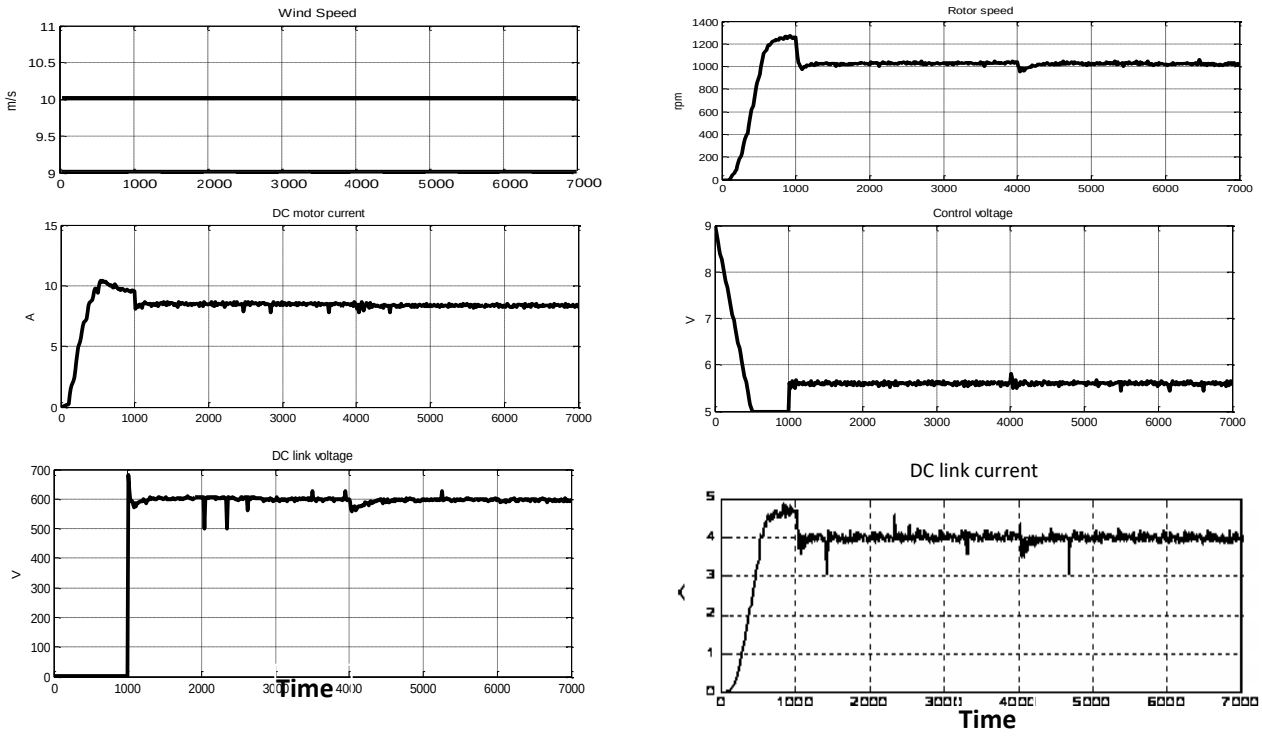

Figure 7. Experimental constant wind speed test result

Figure.7 shows the test result for constant wind speed. The figure shows wind speed, rotor speed, DC motor current, control voltage, DC link current and DC link voltage, respectively. Wind speed is constant along the whole time of the experiment and equal to 10 m/s. All result obtained shows that, after starting period there is no change in the values of all results obtained during this test. Rotor speed is 1000 rpm, DC motor current is 9 A, control voltage is 5.6, V DC link current is 4 A and DC link voltage is 600 V.

4.2. Step increasing

In this case, 60 % step increasing in the wind speed is applied. The initial value of both wind speed and rotor speed is 6 m/sec and 300 rpm respectively. The final wind speed is 10 m/sec. Figure.8 shows Experimental open loop result of WECS for 60 % step increase in wind speed. The figure shows the wind speed, rotor speed, DC motor current, control voltage, DC link voltage and DC link current respectively.

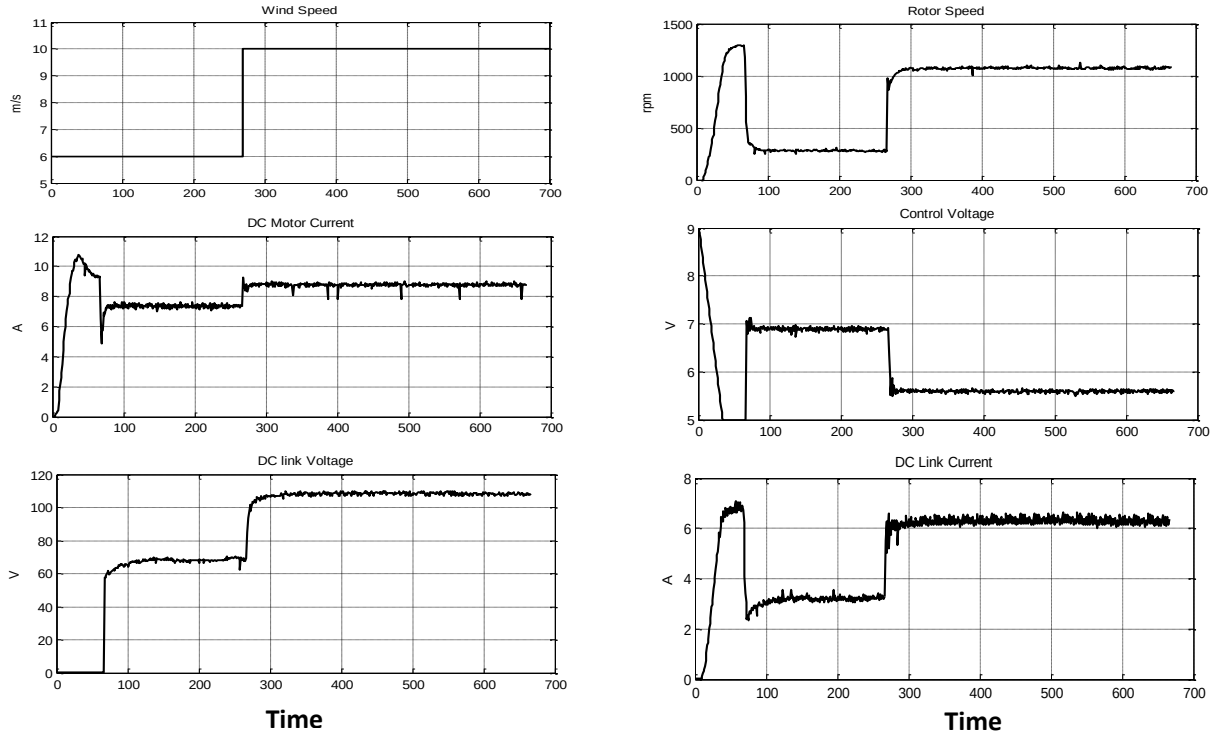

Figure 8. Experimental step increasing test result

Figure.8 shows that the results parameter of the experimental setup has two stage of operation. Experiment starts with wind speed equal to 6 m/s and consequently rotor speed is 300 rpm, DC motor current is 7.5 A, control voltage is 7, V DC link current is 3 A and DC link voltage is 70 V. As the wind speed increased the rotor speed increased to 1100 rpm, DC motor current increased to 9 A, DC link current increased to 6 A and DC link voltage were also increased to 110 V. And the amount of increasing output is relatively to the amount of increasing the wind speed, that's mean the output is governed by the equation of calculating the mechanical power produced by applying the wind speed.

5. Conclusions

In this research, a WTE system is designed and fabricated experimentally using a separately excited DC motor controlled with a half controlled thyristorized converter bridge. Operation of the DC motor is controlled with a current controlled technique using a PI controller. Two groups of tests are carried out to test and reflect the dependency of the proposed system in simulation of WT system. Constant and step increasing in wind speed cases are listed to study the efficiency of using such system. The results reflect the validity of using this system laboratory in addition to its simplicity and dependency.

References

1. Biweta, M., & Mengesha Mamo, D. H. Dynamic Model and Simulation of Wind Energy Conversion System based on Permanent Magnet Synchronous Generator.
2. Bagul, A. C., Kulkarni, A. M., & Dayma, A. S. (2018). Review of Wind Energy Market.
3. Thakur, A., Panigrahi, S., & Behera, R. R. (2016, December). A review on wind energy conversion system and enabling technology. In 2016 International Conference on Electrical Power and Energy Systems (ICEPES) (pp. 527-532). IEEE.

4. Ramos, G., Melo-Lagos, I. D., & Cifuentes, J. (2016). High performance control of a three-phase PWM rectifier using odd harmonic high order repetitive control. Dyna, 83(198), 27-36.
5. Razak, I. S. A., Hashim, R. I. Z. R. Z., & Soid, S. N. M. (2016). A Design of Single Phase Bridge Full-wave Rectifier.
6. Barah, S. S., & Behera, S. (2021, January). An Optimize Configuration of H-Bridge Multilevel Inverter. In 2021 1st International Conference on Power Electronics and Energy (ICPEE) (pp. 1-4). IEEE.
7. Abdelati, M. M. (2014). Design and Implementation of a Viable Power Inverter. In 5th International Conference on Engineering and Sustainability. Islamic University of Gaza, Gaza.
8. Liu, H. (2016). Control design of a single-phase dc/ac inverter for PV applications.
9. Gupta, S. K., & Srivastava, R. K. (2020). A Novel Hybrid Solar-wind Energy Conversion System for Remote Area Electrification. Recent Advances in Electrical & Electronic Engineering (Formerly Recent Patents on Electrical & Electronic Engineering), 13(6), 906-917.
10. Koratagere Srinivasa Raju, B. (2011). Design Optimization Of A Wind Turbine Blade.
11. Michalke, G., & Hansen, A. D. (2010). Modelling and control of variable speed wind turbines for power system studies. Wind Energy: An International Journal for Progress and Applications in Wind Power Conversion Technology, 13(4), 307-322.
12. Karabacak, M., Küçük, T. V., Atmaca, Ö., Kamal, T., & Cantaş, Y. (2018). Design and Implementation of a Wind Turbine Emulator for Wind Energy Conversion Systems. In 7th International Conference on Advanced Technologies (pp. 135-139).
13. Abdallah, M. E., Arafa, O. M., Shaltot, A., & Aziz, G. A. A. (2018). Wind turbine emulation using permanent magnet synchronous motor. Journal of Electrical Systems and Information Technology, 5(2), 121-134.
14. Rifa'i, M., Mandayatma, E., & Putri, R. I. (2020). Speed controller of wind turbine emulator using variable speed drive based on PI method. In IOP Conference Series: Materials Science and Engineering (Vol. 732, No. 1, p. 012059). IOP Publishing.
15. Moussa, I., & Khedher, A. (2020). A Theoretical and Experimental Study of a Laboratory Wind Turbine Emulator using DC-Motor Controlled by an FPGA-Based Approach. Electric Power Components and Systems, 48(4-5), 399-409.
16. Apribowo, C. H. B., & Maghfiroh, H. Fuzzy Logic Controller and Its Application in Brushless DC Motor (BLDC) in Electric Vehicle-A Review. Journal of Electrical, Electronic, Information, and Communication Technology, 3(1), 35-43.
17. Wollz, D. H., da Silva, S. A. O., & Sampaio, L. P. (2020). Real-time monitoring of an electronic wind turbine emulator based on the dynamic PMSG model using a graphical interface. Renewable Energy, 155, 296-308.
18. Beladjine, D. E., Boudana, D., Moualdia, A., Hallouz, M., & Wira, P. (2021, March). A Comparative Study of BLDC Motor Speed Control Using PI and ANN Regulator. In 2021 18th International Multi-Conference on Systems, Signals & Devices (SSD) (pp. 1291-1295). IEEE.